

Explicit and Implicit IDA-PBC Design and Implementation for a Portal Crane

Enrique J. Vidal, Oscar B. Cieza*, Johann Reger*

*Control Engineering Group, Technische Universität Ilmenau, 98684,
Ilmenau, Germany (e-mail: evidals@pucp.edu.pe,
{oscar.cieza, johann.reger}@tu-ilmenau.de)*

Abstract: The interconnection and damping assignment passivity-based control (IDA-PBC) is well-known for regulating the behavior of nonlinear systems. In underactuated mechanical systems (UMSs), its application requires the satisfaction of matching conditions, which in many cases demands to solve partial differential equations (PDEs). Only recently, the IDA-PBC method has been extended to UMSs in implicit representation, where the system dynamics are described by a set of differential-algebraic equations. In some system classes, this implicit model allows to circumvent the PDE obstacle and to construct an output-feedback law. This paper discusses the design and real-system implementation of the total energy shaping IDA-PBC with an optimal local performance for a portal crane system in implicit port-Hamiltonian representation. The implicit controller is compared with the simplified (explicit) IDA-PBC, introduced by Xue and Zhiyong (2017), which also shapes the total energy and avoids PDEs.

Keywords: IDA-PBC, Port-Hamiltonian systems, Implicit systems, Passivity, Portal crane.

1. INTRODUCTION

The purpose of the interconnection and damping assignment passivity-based control (IDA-PBC) technique is to transform a nonlinear system into a closed-loop that takes a port-Hamiltonian (pH) structure with a desired target Hamiltonian. Its application requires to satisfy the so-called matching conditions. In underactuated mechanical systems (UMSs) the IDA-PBC method was first characterized using the explicit pH structure (Ortega et al., 2002), where shaping the energy usually requires the solution of two partial differential equations (PDEs): one for the kinetic energy and one for the potential energy. However, in general, solving these PDEs is not an easy task.

The IDA-PBC has already been tested on portal crane systems. For instance, Banavar et al. (2006) apply a potential energy-shaping IDA-PBC, while Singhal et al. (2006) employ the total energy-shaping IDA-PBC, with constant target inertia matrix. Later, on the basis of the PID-PBC, Donaire et al. (2015) present a method to shape the energy of a class of mechanical systems without solving PDEs and apply their results on a portal crane. Not long ago, Xue and Zhiyong (2017) implement in such a system the simplified IDA-PBC of Ryalat and Laila (2016) which reduces the potential energy PDE to a simple integral by selecting an adequate target inertia matrix. Above research uses the (simplified) planar model except for

(Donaire et al., 2015) where the model is in 3-D. Moreover, all of these approaches use an explicit formulation.

The difference between an explicit and an implicit model relies on the considerations of physical constraints. Thus, complex systems can be modeled as simpler interconnected subsystems, where interconnections (constraints) are described by algebraic equations, forming a set of differential-algebraic equations (DAEs). In this context, Castaños et al. (2013) provide a complete geometric relation between the implicit and explicit port-Hamiltonian representations, concluding that the controller design or implementation is independent of its representation (implicit or explicit). Later, Macchelli (2014) extends the passivity-based control (PBC) theory applied to implicit systems on Dirac structures. Taking a closer look, Cieza and Reger (2019) extend the total energy shaping IDA-PBC technique to implicit UMSs. Their work gives a general method which is not restricted to holonomic systems and does not require a positive definite target inertia matrix. Besides, for some system classes, they can reduce the (energy shaping) PDEs to algebraic equations and devise an output-feedback law.

Until now, the Implicit IDA-PBC technique has remained in a theoretical and simulation framework with no physical implementation. Thus, the main contribution of this work is to work out the results of the implicit control algorithm on a constant rope-length portal crane system and compare these results with that of the simplified (explicit) IDA-PBC from Xue and Zhiyong (2017).

The paper is organized as follows. In Section 2, we briefly recall the implicit and explicit IDA-PBC approaches. Section 3 is devoted to analyzing the explicit planar (2-D) and implicit 3-D models of a portal crane. In Section 4, we apply both methods to the aforesaid system and present a

* The second author acknowledges financial support obtained from: (1) Deutscher Akademischer Austauschdienst (DAAD), Germany, and (2) Programa Nacional de Becas y Crédito Educativo, Peru. The second and third author acknowledge financial support from European Union Horizon 2020 research and innovation program, Marie Skłodowska-Curie grant agreement No.734832.

local linear performance assignment for the implicit controller. Section 5 presents the experimental results. Finally, we draw our conclusions in Section 6.

2. IMPLICIT AND EXPLICIT IDA-PBC FOR UMS

Let us briefly summarize the general formulation of implicit IDA-PBC for UMSs introduced by Cieza and Reger (2019). Consider the implicit pH system¹

$$\begin{bmatrix} \dot{r} \\ \dot{\rho} \end{bmatrix} = \begin{bmatrix} 0 & I_{n_r} \\ -I_{n_r} & 0 \end{bmatrix} \begin{bmatrix} \partial_r^\top \mathcal{H} \\ \partial_\rho^\top \mathcal{H} \end{bmatrix} + \begin{bmatrix} 0 \\ b(r) \end{bmatrix} \lambda + \begin{bmatrix} 0 \\ \mathcal{G}(r) \end{bmatrix} u, \quad (1a)$$

$$b^\top(r) \partial_\rho^\top \mathcal{H} = 0, \quad (1b)$$

$$\mathcal{H}(r, \rho) = \frac{1}{2} \rho^\top \mathcal{M}(r)^{-1} \rho + \mathcal{V}(r)$$

and the desired closed-loop implicit pH system

$$\begin{bmatrix} \dot{r} \\ \dot{\rho} \end{bmatrix} = \begin{bmatrix} 0 & \mathcal{J}(r) \\ -\mathcal{J}^\top(r) & -\mathcal{W}(r, \rho) \end{bmatrix} \begin{bmatrix} \partial_r^\top \mathcal{H}_d \\ \partial_\rho^\top \mathcal{H}_d \end{bmatrix} + \begin{bmatrix} 0 \\ b_d(r) \end{bmatrix} \lambda_d, \quad (2a)$$

$$b_d^\top(r) \partial_\rho^\top \mathcal{H}_d = 0, \quad (2b)$$

$$\mathcal{H}_d(r, \rho) = \frac{1}{2} \rho^\top \mathcal{M}_d(r)^{-1} \rho + \mathcal{V}_d(r), \quad b_d(r) = \mathcal{J}^\top(r) b(r),$$

where $r \in \mathbb{R}^{n_r}$ and $\rho \in \mathbb{R}^{n_\rho}$ are implicit coordinates (position and its canonical momenta, respectively), $u \in \mathbb{R}^{n_u}$ is the input, $\mathcal{G} : \mathbb{R}^{n_r} \rightarrow \mathbb{R}^{n_r \times n_u}$ is the implicit input matrix, $\mathcal{M}, \mathcal{M}_d : \mathbb{R}^{n_r} \rightarrow \mathbb{R}^{n_r \times n_r}$ are the (nominal and desired) nonsingular inertia matrices with $\mathcal{M} \succ 0$, $\mathcal{H}, \mathcal{H}_d : \mathbb{R}^{n_r} \times \mathbb{R}^{n_\rho} \rightarrow \mathbb{R}$ are the Hamiltonians representing (nominal and desired) energy functions, (1b) and (2b) are kinematic constraints, and implicit variables $\lambda, \lambda_d \in \mathbb{R}^{n_\lambda}$ are related to the constraints forces $b(r)\lambda, b_d(r)\lambda_d$ with $b, b_d : \mathbb{R}^{n_r} \rightarrow \mathbb{R}^{n_r \times n_\lambda}$. If (1) is holonomic (integrable constraints), then there exist a function $\phi : \mathbb{R}^{n_r} \rightarrow \mathbb{R}^{n_\lambda}$ such that $\phi(r) = 0$ (zero level set) and $\partial_r^\top \phi(r) = b(r)$.

Definition 1. Let $S(r) := [\mathcal{G}(r) \ b(r)]$. System (1) with holonomic constraints is underactuated if $\text{rank } S < n_r$; else it is fully actuated (Castaños and Gromov, 2016).

To avoid cumbersome notation we will omit the arguments of functions that have been previously defined.

Proposition 2. (Well posedness). Consider the implicit system (1). Then for all $r \in \mathcal{X} := \{r \in \mathbb{R}^{n_r} \mid \text{rank } \Delta = n_\lambda\}$, $\Delta = b^\top \mathcal{M}^{-1} b$, the constrained state-space set $\mathcal{X}_c := \{(r, \rho) \in \mathcal{X} \times \mathbb{R}^{n_\rho} \mid b^\top \partial_\rho^\top \mathcal{H} = 0, \phi(r) = 0\}$ is a regular manifold embedded² in $\mathbb{R}^{n_r} \times \mathbb{R}^{n_\rho}$, and (1) is a system of DAEs with unique solution for λ and differential index 1.

Let us define $\Delta_d := b_d^\top \mathcal{M}_d^{-1} b_d$. Similarly, λ_d has a unique solution for all $r \in \mathcal{X}_d := \{r \in \mathbb{R}^{n_r} \mid \text{rank } \Delta_d = n_\lambda\}$, which is obtained from the hidden constraint $0 = \frac{d}{dt} (b_d^\top \partial_\rho^\top \mathcal{H}_d)$.

Proposition 3. (Implicit IDA-PBC). The implicit feedback $u = u_I(r, \rho)$ with

$$u_I(r, \rho) = S^\dagger (\partial_r^\top \mathcal{H} - \mathcal{J}^\top \partial_r^\top \mathcal{H}_d - \mathcal{W} \partial_\rho^\top \mathcal{H}_d + \mathcal{J}^\top b \lambda_d) \quad (3)$$

transforms the system (1) into (2) for all $r \in \mathcal{X} \cap \mathcal{X}_d$, whenever the implicit matching conditions

¹ We write $\frac{\partial h}{\partial x} = \partial_x h$ or $(\frac{\partial h}{\partial x})^\top = \partial_x^\top h$ for any vector or scalar function $h(x)$. I_n denotes the identity matrix of size n .

² The constrained state space is the space of variables (r, ρ) , while the configuration space (or manifold) is the space of coordinates r .

$$S_\perp (\partial_r^\top (\rho^\top \mathcal{M}^{-1} \rho) - \mathcal{J}^\top \partial_r^\top (\rho^\top \mathcal{M}_d^{-1} \rho) - \mathcal{W}_1 \mathcal{M}_d^{-1} \rho) = 0, \quad (4a)$$

$$S_\perp (\partial_r^\top \mathcal{V} - \mathcal{J}^\top \partial_r^\top \mathcal{V}_d) = 0, \quad (4b)$$

$$S_\perp \mathcal{M}_d \mathcal{M}^{-1} b = 0, \quad (4c)$$

are satisfied.³ Here we denote $S^\dagger = [I_{n_u} \ 0] (S^\top S)^{-1} S^\top$, $\mathcal{J} = \mathcal{M}^{-1} \mathcal{M}_d$, $\mathcal{W}(r, \rho) := \frac{1}{2} \mathcal{W}_1(r, \rho) + S K_u(r) S^\top$, $\mathcal{W}_1 \in \mathbb{R}^{n_r \times n_r}$ with \mathcal{W}_1 linear in ρ , and $K_u \in \mathbb{R}^{(n_u+n_\lambda) \times (n_u+n_\lambda)}$. Define $\mathcal{X}_I = (\{r \in \mathcal{X}_d \mid b_\perp \mathcal{M} \mathcal{M}_d^{-1} \mathcal{M} b_\perp^\top \succ 0\} \times \mathbb{R}^{n_r}) \cap \mathcal{X}_c$. The closed-loop system (2) has a stable equilibrium in $(r^*, 0) \in \mathcal{X}_a = \{x \in \mathcal{X}_I \mid S_\perp \partial_r^\top \mathcal{V} = 0\}$ if⁴

$$r^* = \arg \min_{r \in \mathcal{X}_I} \mathcal{V}_d \quad (5a)$$

is an isolated minimum,

$$0 = \rho^\top \mathcal{M}_d^{-1} \mathcal{W}_1 \mathcal{M}_d^{-1} \rho|_{\mathcal{X}_I}, \quad (5b)$$

and $\text{sym}(K_u) \succeq 0$. Asymptotic stability in r^* is guaranteed if $y_I = \text{sym}(K_u)^{\frac{1}{2}} S^\top \mathcal{M}_d^{-1} \rho$ is a detectable output of (2).

Proposition 4. (Algebraic Implicit IDA-PBC). Let system (1) be holonomic and assume it possesses constant \mathcal{M} , $\partial_r^\top \mathcal{V}$, and polynomial \mathcal{G}, ϕ . Feedback (3) stabilizes the closed-loop at $(r^*, 0)$ if there are

- C1. a vector $\mu^* \in \mathbb{R}^{n_\lambda}$,
- C2. a symmetric matrix $A \in \mathbb{R}^{(n_r-n_\lambda) \times (n_r-n_\lambda)}$, $A \succ 0$,
- C3. a matrix $C \in \mathbb{R}^{(n_r-n_\lambda) \times n_\lambda}$,
- C4. a non-singular matrix $D \in \mathbb{R}^{n_\lambda \times n_\lambda}$, and
- C5. a function $\bar{S} : \mathbb{R}^{n_r} \rightarrow \mathbb{R}^{(n_u+n_\lambda) \times n_\psi}$, $n_\psi \leq n_u + n_\lambda$,

such that (4c) and

$$S_\perp (\partial_r^\top \mathcal{V} + \mathcal{M} Z_c D b^* \mu^*) = 0, \quad (6a)$$

$$\partial_r (S \bar{S}_i) \mathcal{M}^{-1} \mathcal{M}_d - \mathcal{M}_d \mathcal{M}^{-1} \partial_r^\top (S \bar{S}_i) = 0, \quad (6b)$$

$$Z_\perp A b_\perp^* (\partial_r (b \mu^*)|_{r=r^*}) b_\perp^{\top} A Z_\perp^\top \succ 0 \quad (6c)$$

hold with \bar{S}_i the i th column of \bar{S} , $b^* := b(r^*)$, $\tilde{r} := r^* - r$,

$$\mathcal{M}_d = \mathcal{M} B^* \begin{bmatrix} A + CDC^\top CD \\ DC^\top & D \end{bmatrix} B^{*\top} \mathcal{M}, \quad B^{*\top} = \begin{bmatrix} b_\perp^* \\ b^* \end{bmatrix},$$

$$\mathcal{V}_d = \frac{1}{2} \psi^\top K_\psi \psi + \tilde{r}^\top b^* \mu^*, \quad \psi = \int_{r^*}^r \bar{S}_i^\top(s) S^\top(s) \mathcal{M}_d^{-1} \mathcal{M} ds,$$

$K_\psi = K_\psi^\top \succ -Z^\dagger (Z_a - Z_a Z_\perp^\top (Z_\perp Z_a Z_\perp^\top)^{-1} Z_\perp Z_a) Z^{\dagger\top}$, $Z_c = b_\perp^{\top} C + b^*$, $Z = [I_{n_r-n_\lambda} \ -C] B^{*-1} \mathcal{M}^{-1} S(r^*) \bar{S}(r^*)$ is full rank, $Z_a = A b_\perp^* (\partial_r (b \mu^*)|_{r=r^*}) b_\perp^{\top} A$, $Z^\dagger = (Z^\top Z)^{-1} Z^\top$, \mathcal{W}_1 fulfills $\mathcal{W}_1^\top [S_\perp^\top \mathcal{M}_d^{-1} \rho] = 0$, and $\text{sym}(K_u) \succeq 0$. Moreover, if $y_I = \text{sym}(K_u)^{\frac{1}{2}} S^\top \mathcal{M}_d^{-1} \rho$ is a detectable output of (2), then r^* is asymptotically stable.

Proposition 5. (Output-feedback). Let the conditions of Prop. 4 be fulfilled with $S \bar{S} = \mathcal{G}$ and $\mathcal{W}_1 = 0$. If in addition $b_\perp \mathcal{M}_d \mathcal{M}^{-1} b = 0$, then the new control law $u = u_N(r, \xi)$,

$$u_N(r, \xi) = S^\dagger (\partial_r^\top \mathcal{H} - \mathcal{J}^\top \partial_r^\top \mathcal{V}_d - \mathcal{G} \bar{K}_u (\xi + \psi(r))), \quad (7a)$$

$$\dot{\xi} = -\Lambda_\xi(r) \bar{K}_u (\xi + \psi(r)), \quad (7b)$$

with $\bar{K}_u = \bar{K}_u^\top$, $\text{sym}(\Lambda_\xi) \succ 0$, $\xi \in \mathbb{R}^{n_u}$, $\Lambda_\xi, \bar{K}_u \in \mathbb{R}^{n_u \times n_u}$, and \mathcal{H}_d as in Prop. 4, stabilizes the system at $(r^*, 0)$. The closed-loop is asymptotically stable at r^* if $y_N = \mathcal{G}^\top \mathcal{M}_d^{-1} \rho$ is a detectable output of (2).

³ We write the subscript \perp for any matrix F to represent its full rank left annihilator, i.e., $F_\perp F = 0$.

⁴ In what follows, $\text{sym}(A) := A + A^\top$, for any square matrix A .

In Propositions 2–5 we have summarized the IDA-PBC methodology for implicit pH systems with holonomic constraints. Besides, if system (1) and (2) have no constraints, namely, (1b) and (2b), we can simply rewrite them as

$$\begin{bmatrix} \dot{q} \\ \dot{p} \end{bmatrix} = \begin{bmatrix} 0 & I_{n_q} \\ -I_{n_q} & 0 \end{bmatrix} \begin{bmatrix} \partial_q^\top H \\ \partial_p^\top H \end{bmatrix} + \begin{bmatrix} 0 \\ G(q) \end{bmatrix} u, \quad \text{and} \quad (8)$$

$$\begin{bmatrix} \dot{q} \\ \dot{p} \end{bmatrix} = \begin{bmatrix} 0 & J \\ -J^\top & -W \end{bmatrix} \begin{bmatrix} \partial_q^\top H_d \\ \partial_p^\top H_d \end{bmatrix}, \quad (9)$$

respectively. Thus, the model is defined by means of the (explicit) generalized coordinates q and momenta p , where $H(q, p) = \frac{1}{2} p^\top M(q)^{-1} p + V(q)$, $H_d(q, p) = \frac{1}{2} p^\top M_d(q)^{-1} p + V_d(q)$ and $M, M_d \succ 0$. The following proposition recalls the standard IDA-PBC for UMSs as presented in (Donaire et al., 2016).

Proposition 6. (IDA-PBC). Feedback $u = u_E(q, p)$ with

$$u_E(q, p) = (G^\top G)^{-1} G^\top (\partial_q^\top H - J^\top \partial_q^\top H_d - W \partial_p^\top H_d) \quad (10)$$

transforms system (8) into the desired system (9) whenever the kinetic and potential matching conditions

$$G_\perp (\partial_q^\top (p^\top M^{-1} p) - J^\top \partial_q^\top (p^\top M_d^{-1} p) - W_1 \partial_p^\top H_d) = 0, \quad (11a)$$

$$G_\perp (\partial_q^\top V - J^\top \partial_q^\top V_d) = 0 \quad (11b)$$

are satisfied with $J = M^{-1} M_d$ and $W = \frac{1}{2} W_1(q, p) + G K_v G^\top$, for W_1 linear in p . The closed loop system is stable in $(q^*, 0)$ with $q^* \in \{q \mid G_\perp \partial_q^\top V = 0\}$ if $q^* = \arg \min V_d$ is an isolated minimum, M_d is positive definite, $\text{sym}(K_v) \succ 0$, and⁵

$$\partial_p H_d W_1 \partial_p^\top H_d = 0. \quad (11c)$$

Moreover if $y_E := G^\top \partial_p^\top H_d$ is a detectable output of (9), then the equilibrium is asymptotically stable.

Observe that the matching conditions (11) and control law (10) of the conventional (explicit) IDA-PBC for an UMS are a specific case ($S = G$, $q = r$, $p = \rho$, $M_d = M_d$, $J = J$, $W = W$, etc.) of the implicit IDA-PBC presented in Prop. 3.

3. PORTAL CRANE MODEL

This work focuses on the portal crane system shown in Fig. 1a, where the support mechanism (frame) is fastened to the floor. On the top, a set of girders and belts move the bridge of mass m_b and the trolley of mass m_t along the x -axis. The trolley, which is mounted under the bridge, is restricted to move in the y -direction. A basket hangs from a winch or rope drum, and thus it can move in the z -direction varying its length l . A load can be attached to the basket in various ways and then transported with it. In the following, we refer to the basket and the additional weight as the payload of mass m_p . The assumptions below are considered throughout this work.

- A1. The rope mass is negligible.
- A2. The payload is a point mass.
- A3. The rope length $l > 0$ is fixed.
- A4. The payload air friction is negligible.

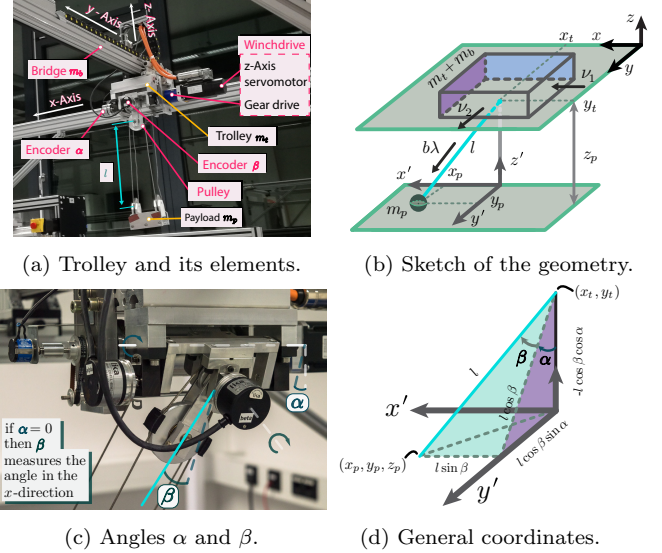


Fig. 1. Physical configuration of the portal crane system.

3.1 3-D Implicit Model

The schematic view of the portal crane is given in Fig. 1b, where we describe the trolley position with $r_t := \text{vec}(x_t, y_t)$, the payload relative position with $r_p := \text{vec}(x_p, y_p, z_p)$, and the trolley external forces (actuators) on the x - and y -axis with $\nu := \text{vec}(\nu_x, \nu_y)$. The selected coordinates lead to the holonomic constraint

$$\phi := \frac{1}{2} (x_p^2 + y_p^2 + z_p^2 - l^2) = 0. \quad (12)$$

To measure real positions, the system is equipped with encoders in x_t, y_t, l, α and β , where the geometric relation shown in Fig. 1c–1d results in

$$x_p = l \sin \beta, \quad y_p = l \cos \beta \sin \alpha, \quad z_p = -l \cos \beta \cos \alpha. \quad (13)$$

Following assumptions A1–A2, we may now calculate the kinetic and potential energy as

$$\begin{aligned} \bar{\mathcal{T}} &= \frac{m_t + m_b}{2} \dot{x}_t^2 + \frac{m_t}{2} \dot{y}_t^2 + \frac{m_p}{2} ((\dot{x}_t + \dot{x}_p)^2 + (\dot{y}_t + \dot{y}_p)^2 + \dot{z}_p^2), \\ \bar{\mathcal{V}} &= m_p g_r z_p, \end{aligned}$$

where g_r is the gravity constant. From assumptions A3–A4 and coordinates $r := \text{vec}(r_p, r_t)$, the Lagrange equations with external forces $\bar{\mathcal{G}}u$ and constrains (12) gives

$$\begin{bmatrix} \bar{\mathcal{M}}_1 & \bar{\mathcal{M}}_2 \\ \bar{\mathcal{M}}_2^\top & \bar{\mathcal{M}}_3 \end{bmatrix} \begin{bmatrix} \ddot{r}_p \\ \ddot{r}_t \end{bmatrix} + \begin{bmatrix} 0 \\ \mathcal{R}_t \dot{r}_t \end{bmatrix} + \begin{bmatrix} \partial_{r_p}^\top \bar{\mathcal{V}} \\ \partial_{r_t}^\top \bar{\mathcal{V}} \end{bmatrix} = \begin{bmatrix} \partial_{r_p}^\top \phi \\ \partial_{r_t}^\top \phi \end{bmatrix} \bar{\lambda} + \begin{bmatrix} 0_{3 \times 2} \\ I_2 \end{bmatrix} \nu,$$

where $\bar{\mathcal{M}}_2 = m_p \begin{bmatrix} I_2 \\ 0_{1 \times 2} \end{bmatrix}$, $\bar{\mathcal{M}}_1 = m_p I_3$, $\bar{\mathcal{M}}_3 = \text{diag}(m_t + m_b + m_p, m_t + m_p)$, and \mathcal{R}_t are the bridge-trolley frictions. By using partial feedback linearization (PFL) (Spong, 1994) with $u = \ddot{r}_t$ (trolley acceleration), it follows that

$$\begin{bmatrix} \ddot{r}_p \\ \ddot{r}_t \end{bmatrix} = \begin{bmatrix} m_p^{-1} \partial_{r_p}^\top \bar{\mathcal{V}} \\ 0 \end{bmatrix} + \begin{bmatrix} m_p^{-1} \partial_{r_p}^\top \phi \\ 0 \end{bmatrix} \bar{\lambda} + \begin{bmatrix} -m_p^{-1} \bar{\mathcal{M}}_2 \\ I_2 \end{bmatrix} u, \quad (14a)$$

$$\nu = f_1(r, \dot{r}, \bar{\lambda}) + f_2(r)u, \quad (14b)$$

for some functions f_1 and f_2 . Now, we can rewrite (14a) as (1) with $\mathcal{H}(r, \rho) := \frac{1}{2} \rho^\top \rho + g_r z_p$, $b = \text{vec}(x_p, y_p, z_p, 0, 0)$, $\mathcal{G}^\top = \begin{bmatrix} -1 & 0 & 0 & 1 & 0 \\ 0 & -1 & 0 & 0 & 1 \end{bmatrix}$ and $\lambda = \frac{1}{m_p} \bar{\lambda}$. Note that $\mathcal{M} = I_5$ which implies $\dot{r} = \rho$.

⁶ We write $\text{vec}(x_1, x_2, \dots, x_n) = [x_1^\top \ x_2^\top \ \dots \ x_n^\top]^\top$ for any scalars or column vectors x_1, x_2, \dots, x_n .

⁵ Skew-symmetry of W_1 is a sufficient condition for (11c).

Our laboratory setup includes a PID + Feedforward trolley velocity loop as shown in Fig. 2. This inner loop with an additional integrator before ν yields a system which can be approximated as (14a). Consequently, the integrator with PID + Feedforward is also an approximation of (14b), and it avoids the necessity to estimate the system masses (e.g. trolley, payload, bridge), inertias, and frictions.

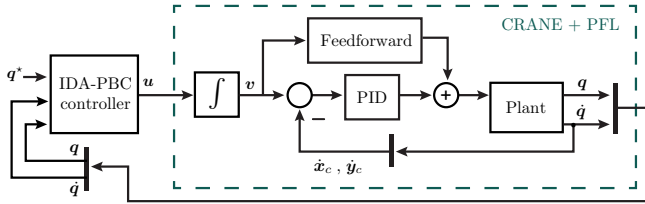


Fig. 2. IDA-PBC block diagram

3.2 Planar Explicit Model

To model the real crane of Fig. 1 in 2-D, the following assumption is required.

A5. The angles β and α are sufficiently small s.t. the axes (x and y) are approximately decoupled.

The dynamics of this reduced system with PFL can be found in (Xue and Zhiyong, 2017) and is given by two systems of the form of (8), where $H(q, p) = \frac{1}{2}p^\top p - \bar{g} \cos q_1$, $G(q) = \text{vec}(-a \cos q_1, 1)$, $a = 1/l$, and $\bar{g} = g_r/l$. Besides, the first system has $q = \text{vec}(q_1, q_2) = \text{vec}(\beta, x_t)$ and $u = \ddot{x}_t$, while the second one has $q = \text{vec}(q_1, q_2) = \text{vec}(\alpha, y_t)$ and $u = \ddot{y}_t$. Similar to the 3-D model with PFL we have $M = I_2$ and $\dot{q} = p$.

4. IDA-PBC IN THE PORTAL CRANE

4.1 State Feedback Implicit IDA-PBC

We now use Prop. 3 to synthesize controller u_I . Since our desired position is $r^* = \text{vec}(0, 0, -l, x_c^*, y_c^*)$, we see that $b^* = \text{vec}(0, 0, -l, 0, 0)$. Selecting $C = 0_{4 \times 1}$,

$$S_\perp = \begin{bmatrix} -z_p & 0 & x_p & -z_p & 0 \\ 0 & -z_p & y_p & 0 & -z_p \end{bmatrix} \text{ and } b_\perp^* = l \begin{bmatrix} I_2 & 0_{2 \times 1} & 0_2 \\ 0_2 & 0_{2 \times 1} & I_2 \end{bmatrix},$$

we obtain $Z_c = b^*$. From (4c) and (6a) for arbitrary x_p, y_p and z_p , it follows that $\mu^* = \frac{g_r}{Dl^3}$ and

$$A = \begin{bmatrix} a_1 & e_1 & D - a_1 & -e_1 \\ e_1 & a_2 & -e_1 & D - a_2 \\ D - a_1 & -e_1 & d_1 & e_2 \\ -e_1 & D - a_2 & e_2 & d_2 \end{bmatrix},$$

where a_i, d_i, e_i and D are arbitrary constants s.t. $A \succ 0$. In the next step we choose $S\bar{S} = \mathcal{G}$, which clearly fulfills (6b) because \mathcal{G} is constant. Then, we calculate Z and pick $Z_\perp = \begin{bmatrix} 1 & 0 & 1 & 0 \\ 0 & 1 & 0 & 1 \end{bmatrix}$ obtaining that (6c) is satisfied for any $D > 0$. In the following, to simplify analysis, we set $e_i = 0$ and $\mathcal{W}_1 = 0_{5 \times 5}$. At this point, we are able to calculate

$$\psi = \begin{bmatrix} -\frac{D(x_t^* - x_t) + x_p(D - a_1 + d_1)}{l^2 \gamma_1} \\ -\frac{D(y_t^* - y_t) + y_p(D - a_2 + d_2)}{l^2 \gamma_2} \end{bmatrix}.$$

where $\gamma_i = d_i a_i - D^2 + 2D a_i - a_i^2$. Finally, we select $K_\psi = \text{diag}(K_{\psi 1}, K_{\psi 2})$, $K_{\psi i} > 0$, $K_u = \text{diag}(K_{u1}, K_{u2}, 0)$, $K_{ui} > 0$, and $A \succ 0$. Now, all elements of the control law (3) are on hand.

4.2 Output Feedback Implicit IDA-PBC

If additionally, $a_i = D$, then $b_\perp \mathcal{M}_d \mathcal{M}^{-1} b = 0$ holds and Prop. 5 can be used selecting $K_{\psi i} > 0$, $\text{sym}(\Lambda_\xi) \succ 0$ and $\bar{K}_u = \text{diag}(\bar{K}_{u1}, \bar{K}_{u2})$, $\bar{K}_{ui} > 0$.

4.3 Explicit IDA-PBC Control Law

Xue and Zhiyong (2017) applied the simplified IDA-PBC introduced by Ryalat and Laila (2016) on the portal crane model of Section 3.2. However, their feedback law has the velocity \dot{q}_2 in the denominator, and thus, it is not well-defined for all $(q, p) \in \mathcal{E} = \{(q, p) \mid \dot{q}_2 = 0\}$. Additional inspection shows that the kinetic matching condition is also not satisfied for all $(q, p) \in \mathcal{E}$. To avoid the aforementioned problems, we redesign the controller searching for new M_d and V_d .

Let $G_\perp = [1 \ a \cos q_1]$, $W_1 = \begin{bmatrix} 0 & -s \\ s & 0 \end{bmatrix}$, $s = s_1(q_1)\eta_1 + s_2(q_1)\eta_2$, $M_d = \begin{bmatrix} m_1(q_1) & m_2(q_1) \\ m_2(q_1) & m_3 \end{bmatrix}$, and $\eta := \partial_p^\top H_d = \text{vec}(\eta_1, \eta_2)$, then (11a) can be reduced to

$$K_1 \eta^\top \partial_{q_1} (M_d) \eta + 2G_\perp \begin{bmatrix} 0 & -s \\ s & 0 \end{bmatrix} \eta = 0, \quad (15)$$

where $K_1 = m_1(q_1) + a m_2(q_1) \cos q_1$. Equation (15) has a solution for arbitrary η_1 and η_2 if and only if $s_2(q_1) = 0$,

$$K_1 \partial_{q_1} (m_1) + 2a s_1(q_1) \cos q_1 = 0, \quad \text{and} \quad (16a)$$

$$K_1 \partial_{q_1} (m_2) - s_1(q_1) = 0. \quad (16b)$$

We can simplify the potential energy PDE (11b) to a simple integral by selecting $m_2(q_1) = -a m_3 \cos q_1$. Now we can solve (16), obtaining $s_1 = K_1 a m_3 \sin(q_1)$ and $m_1 = a^2 m_3 \cos(q_1)^2 + c_1$ for some constant c_1 . Therefore,

$$M_d = \begin{bmatrix} a^2 m_3 \cos(q_1)^2 + c_1 & -a m_3 \cos q_1 \\ -a m_3 \cos q_1 & m_3 \end{bmatrix}, \quad (17)$$

$$V_d = -\frac{\bar{g} \cos q_1}{c_1} + \Upsilon(q_2), \quad (18)$$

with Υ being an arbitrary function. Let $\Upsilon := 1/2 K_p (q_2 - q_2^*)^2$, then it is straightforward to proof that $M_d \succ 0$ and $q^* = (0, q_2^*)$ is a strict local minimum of V_d if $K_p > 0$, $c_1 > 0$, and $m_3 > 0$. Finally, choosing $K_v > 0$, we see that the (explicit) IDA-PBC controller (10) is reduced to

$$u_E(q, \dot{q}) = \frac{m_3 \sin(q_1)}{c_1} (\dot{q}_2 q_1 a^2 \cos q_1 + a \dot{q}_1^2 + \bar{g} a \cos q_1) + K_p m_3 (q_2^* - q_2) - \frac{K_v \dot{q}_2}{m_3}. \quad (19)$$

Clearly, the previous controller is well defined for any \dot{q}_2 and is independent of any mass.

4.4 Local Linear Performance

Using Proposition 5 of (Cieza and Reger, 2019) we can reduce⁷ the implicit (holonomic) system (14a) in the

⁷ The coordinate reduction eliminates the constraint $b^\top \partial_p \mathcal{H} = 0$ and constraint forces $b\lambda$.

form of (1) to an explicit pH representation of the form of (8), where $q = \text{vec}(\beta, \alpha, x_t, y_t)$, $M = (\partial_q^\top h)\mathcal{M}(\partial_q h)$, $\rho = \dot{r} = (\partial_q^\top h)M^{-1}p$, $G = (\partial_q^\top h)\mathcal{G}$, $V = \mathcal{V}(h(q))$, and the geometric relation $r = h(q)$ is defined by (13).⁸ Note that the implicit inertia matrix \mathcal{M} is constant, while the explicit one, M , is not. Let $x := \text{vec}(q, p)$. The linearization of the portal-crane system with controller (3) about the point $x = x^* := \text{vec}(\beta, \alpha, x_t^*, y_t^*, 0, 0, 0, 0)$ is

$$\dot{\tilde{x}} = (A_r + B_r K_I)\tilde{x},$$

where $\tilde{x} = x - x^*$, $\bar{u}_I(q, p) = u_I(h(q), (\partial_q^\top h)M^{-1}p)$,

$$A_r = \begin{bmatrix} 0 & I_4 \\ -I_4 & 0 \end{bmatrix} \bigg|_{x=0} \frac{\partial^2 H}{\partial x^2}, \quad B_r = \begin{bmatrix} 0_{4 \times 2} \\ G(0) \end{bmatrix},$$

$$K_I = \partial_x \bar{u}_I|_{x=0} = \begin{bmatrix} k_{11} & 0 & k_{12} & 0 & k_{13} & 0 & k_{14} & 0 \\ 0 & k_{21} & 0 & k_{22} & 0 & k_{23} & 0 & k_{24} \end{bmatrix}$$

$$k_{i1} = \frac{K_{\psi i}(D - a_i + d_i)}{l\gamma_i} + \frac{a_i g_r}{D} - g_r, \quad k_{i2} = -\frac{DK_{\psi i}}{l^2\gamma_i},$$

$$k_{i3} = \frac{K_{ui}(D - a_i + d_i)}{l^3\gamma_i}, \quad k_{i4} = -\frac{K_{ui}D}{l^2\gamma_i}.$$

Since the pair (A_r, B_r) is controllable for any $l > 0$, we can easily set an LQR local optimal performance to our controller (3) by solving a_i, d_i, D, K_ψ and K_u from $-K_{lqr} = K_I$, where the LQR feedback is $u_{lqr} = -K_{lqr}\tilde{x}$.⁹

Similarly, linearization of the 2-D model (see Section 3.2) with $x := \text{vec}(q_1, q_2, \dot{q}_1, \dot{q}_2)$ and the explicit IDA-PBC controller (19) yields

$$K_E = \partial_x u_E|_{x=0} = \begin{bmatrix} \frac{a\bar{g}m_3}{c_1} & -K_p m_3 & 0 & -\frac{K_v}{m_3} \end{bmatrix}.$$

In comparison, the presence of 0 in the matrix K_E prevents to set an arbitrary LQR local performance, which is a disadvantage of (19) with respect to (3).

5. EXPERIMENTAL RESULTS

Figures 3–5 show experimental step responses with initial conditions $x_t = y_t = \beta = \alpha = \dot{x}_t = \dot{y}_t = \dot{\beta} = \dot{\alpha} = 0$ under five control actions: two implicit full state-feedback IDA-PBC (u_{I1} and u_{I2}), an implicit output-feedback IDA-PBC (u_N), an explicit full state-feedback IDA-PBC (u_E), and an LQR (u_{lqr}). To compare the u_{lqr} and the implicit law u_I we assign the same local performance, i.e., $-K_{lqr} = K_I$, and rename u_I as u_{I1} . Here u_{lqr} is obtained from $A_r, B_r, Q_{lqr} = \text{diag}(400, 400, 100, 100, 10, 10, 1, 1)$, and $R_{lqr} = I_2$. Since the explicit controller u_E does not allow an arbitrary local optimal performance or pole assignment, see Section 4.4, we choose the parameters of u_I s.t. $K_E = [k_{i1} \ k_{i2} \ k_{i3} \ k_{i4}]$, and call it u_{I2} . The parameters of the IDA-PBC controllers are shown in Table 1, where $g_r = 9.81 \text{ m/s}^2$, $l = 1 \text{ m}$, $m_p = 4.975 \text{ kg}$.

First, we observe that all controllers achieve asymptotic stability of the desired position. Besides, since the crane angles β and α are rather small ($-10^\circ < \alpha, \beta < 10^\circ$), we have a very similar behavior for the pairs u_{I1} - u_{lqr} and u_E - u_{I2} . Clearly, the optimal local performance allows a faster settling time and smaller overshoot of u_{I1}

⁸ The reduction is well-defined for $\alpha, \beta \in]-\frac{\pi}{2}, \frac{\pi}{2}[$, i.e., $z_p < 0$.

⁹ Setting the weighting matrices Q_{lqr} and R_{lqr} to be diagonal, produces a K_{lqr} with the same structure (position of zeros) as K_I .

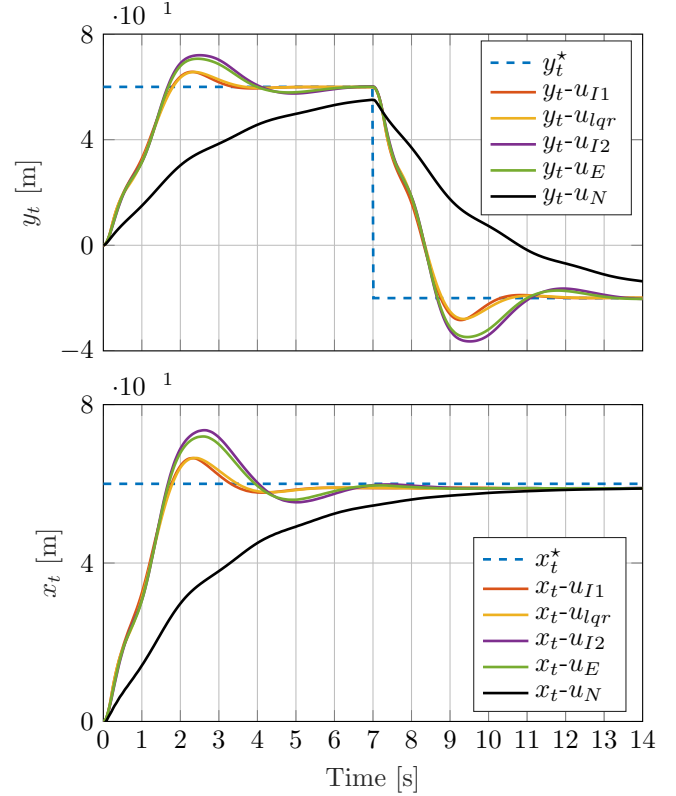


Fig. 3. Crane response: signals x_t and y_t .

and u_{lqr} with respect to u_E . The output-feedback law requires the additional parameter restriction $a_i = D$, so it yields the slowest settling time, but avoids any velocity measurement. Finally, note that the implementation of the implicit IDA-PBC does not depend on the linearization or

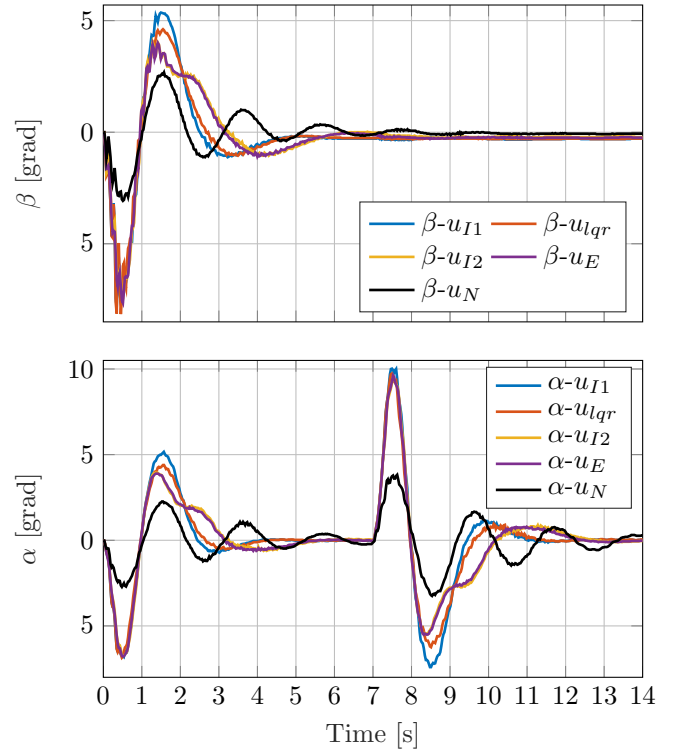


Fig. 4. Crane response: signals β and α .

assumption A5. Consequently, it may allow a larger region of attraction (compared with the local u_{lqr} and u_E).

Table 1. Implicit and explicit IDA-PBC parameters.

		u_N	u_{I1}	u_{I2}	u_E
Parameter	a_i	12	3.2005	3	-
	e_i	0	0	0	-
	d_i	29	2.2671	2	-
	D	12	1	1	-
	μ^*	$g_r/12$	g_r	g_r	-
	K_{ui}	-	19.67	8.57	-
	$K_{\psi i}$	0.0045	24.138	12.6	-
	\bar{K}_{ui}	175	-	-	-
	Λ_ξ	$0.10I_2$	-	-	-
	m_3	-	-	-	0.42
	c_1	-	-	-	$a^2 m_3$
	K_v	-	-	-	1.8
	K_p	-	-	-	15

6. CONCLUSION

Explicit and implicit IDA-PBC approaches are designed and implemented successfully on an experimental portal crane system. Both methods shape the total energy without solving PDEs. The simplified (explicit) IDA-PBC uses a 2-D model, which is obtained under small angle assumption (relative position of the payload w.r.t. the trolley). In contrast, the implicit IDA-PBC uses a 3-D model, avoiding the previous requirement.

On the other hand, we found a significant implementation flaw in the simplified IDA-PBC of Xue and Zhiyong (2017) and solve it by picking a new target Hamiltonian. The application of this method in the portal crane with a 3-D

model is not as straightforward as the one modeled in 2-D. Therefore, we restrict this method to 2-D and apply the feedback in each axis (x and y) as if they were decoupled.

Finally, we compare five control actions: an LQR, an implicit state-feedback IDA-PBC tuned to have the same local behavior as the LQR, a simplified (explicit) IDA-PBC, an implicit state-feedback IDA-PBC tuned to behave locally as the explicit one, and an output-feedback implicit IDA-PBC. The results give favour to the implicit IDA-PBC instead of the simplified explicit one.

REFERENCES

- Banavar, R., Kazi, F., Ortega, R., and Manjarekar, N. (2006). The IDA-PBC methodology applied to a gantry crane. In *Proceedings of the Mathematical Theory of Networks and Systems*, 143–147.
- Castaños, F. and Gromov, D. (2016). Passivity-based control of implicit port-Hamiltonian systems with holonomic constraints. *Systems & Control Letters*, 94, 11–18.
- Castaños, F., Gromov, D., Hayward, V., and Michalska, H. (2013). Implicit and explicit representations of continuous-time port-Hamiltonian systems. *Systems & Control Letters*, 62(4), 324–330.
- Cieza, B.O. and Reger, J. (2019). IDA-PBC for underactuated mechanical systems in implicit port-Hamiltonian representation. *European Control Conference*, 614–619.
- Donaire, A., Mehra, R., Ortega, R., Satpute, S., Romero, J.G., Kazi, F., and Singh, N.M. (2015). Shaping the energy of mechanical systems without solving partial differential equations. In *American Control Conference (ACC)*, 1351–1356.
- Donaire, A., Ortega, R., and Romero, J.G. (2016). Simultaneous interconnection and damping assignment passivity-based control of mechanical systems using dissipative forces. *Systems & Control Letters*, 94, 118–126.
- Macchelli, A. (2014). Passivity-based control of implicit port-Hamiltonian systems. *SIAM Journal on Control and Optimization*, 2422–2448.
- Ortega, R., Spong, M.W., Gómez-Estern, F., and Blankenstein, G. (2002). Stabilization of a class of underactuated mechanical systems via interconnection and damping assignment. *IEEE Transactions on Automatic Control*, 1218–1233.
- Ryalat, M. and Laila, D.S. (2016). A simplified IDA-PBC design for underactuated mechanical systems with applications. *European Journal of Control*, 27, 1–16.
- Singhal, R., Patayane, R., and Banavar, R.N. (2006). Tracking a trajectory for a gantry crane: Comparison between IDA-PBC and direct Lyapunov approach. In *2006 IEEE International Conference on Industrial Technology*, 1788–1793.
- Spong, M.W. (1994). Partial feedback linearization of underactuated mechanical systems. In *International Conference on Intelligent Robots and Systems (IROS)*, 314–321.
- Xue, L. and Zhiyong, G. (2017). Control of underactuated bridge cranes: A simplified IDA-PBC approach. In *2017 11th Asian Control Conference (ASCC)*, 717–722.

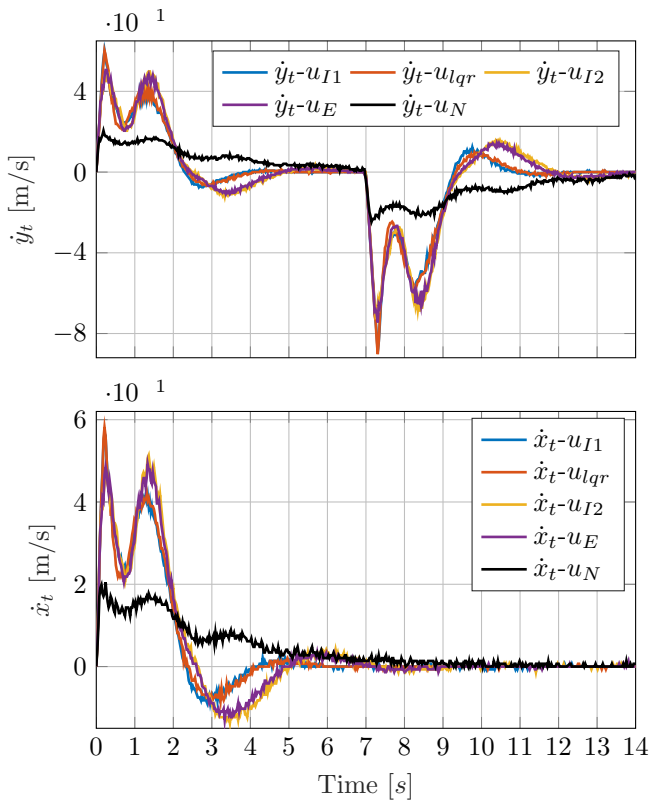


Fig. 5. Crane response: signals \dot{x}_t and \dot{y}_t .